



## Deposition and structuring of Ag/AgCl electrodes inside a closed polymeric microfluidic system for electroosmotic pumping

F. Heuck, P. van der Ploeg, U. Staufer\*

Micro and Nanoengineering Laboratory, TU Delft, Delft 2628CD, The Netherlands

### ARTICLE INFO

Article history:  
Available online xxxxx

Keywords:  
Electroosmotic pump  
Ag/AgCl electrodes  
Electroless deposition  
Microfluidic stopvalve

### ABSTRACT

The design, fabrication and analysis of a low voltage electroosmotic (eo) pump with integrated Ag/AgCl electrodes are shown. The fabrication was based on casting the hydrophilic polymer NOA63, capping the NOA63 trenches with a glass-slide and subsequently depositing Ag/AgCl electrodes by a flow of electroless solution and structuring the electrodes by microfluidic stopvalves. The herewith obtained eo pump embedded into the microfluidic system had a capillary cross-section of  $65 \mu\text{m} \times 55 \mu\text{m}$  and its flow rate was determined to be  $0.12 \text{ nl s}^{-1} \text{ V}^{-1} U_{eh}$  within the range of applied voltages  $U_{eh}$  from  $-1.5$  up to  $1.5 \text{ V}$ .  
© 2011 Published by Elsevier B.V.

### 1. Introduction

In microfluidics, electroosmotic (eo) pumps take advantage of an electric field induced movement of the Debye layer of free charges in a liquid parallel to a charged surface [1,2]. Since these pumps do not require any mechanically moving parts to propel the liquid, they have a high potential for miniaturization and high density integration [1,2]. Generally encountered problem with designing and miniaturizing eo pumps is the coupling of the electrical current into the ionic solution. For this purpose, platinum (Pt) electrodes are commonly used. The electrochemical reaction at the Pt electrodes initiates electrolysis of the liquid into gas. Several methods to avoid mixing of the electrolyzed gases with the functional fluidic system have been reported. Brask et al. [3] used a hybrid approach for the current coupling by assembling an ion exchange membrane between the electrodes and the eo pump. In another approach we suggested to use a gas–liquid-separator to part the electrolyzed gas from the liquid [1,2]. However, electrodes like silver/silver chloride (Ag/AgCl) have the outstanding advantage that during pumping the electrochemical reaction transforms Ag into AgCl and vice versa, hence avoiding the inherent gas bubbles of electrolysis. In addition, Ag/AgCl electrodes are the most common and well understood electrodes for biological and chemical measurements [4]. Here, we present the fabrication of an eo pump with integrated Ag/AgCl electrodes a polymeric, fluidic system. The suggested process provides a quick and cheap alternative to standard bulk silicon micromachining. Following the approach from Dupont et al. [4,5], the capillaries of the microfluidic system were fabricated out of the hydrophilic polymer NOA63. Afterwards,

the Ag/AgCl electrodes were deposited and structured in a similar way to the previously reported electroless process [6]. This allowed the fabrication and the subsequent analysis of an eo pump embedded in a polymeric microfluidic system.

### 2. Design and process flow

The layout of this design was chosen to obtain a better understanding of the fabrication of the polymeric microfluidic system, the electroless AgCl electrode deposition and structuring, as well as, the performance of the Ag/AgCl electrodes for eo pumping. For the layout, a symmetric microfluidic system was chosen with the eo pump in its center, see Fig. 1a. Large reservoirs provided fluidic and electrical connection to the microfluidic system. These four reservoirs were designed into two pairs, where each pair is linked by one capillary representing one electrode. These two electrode capillaries are connected with each other in their center by the eo pump.

The process presented here was intended for a cheap, quick and easy fabrication using a polymer based microfluidic chip fabrication. As suggested by Dupont et al. [4,5], a hydrophilic microfluidic system, made out of NOA63,<sup>1</sup> can be fabricated following the sequence: (a) photolithographical structuring of a SU8<sup>2</sup> layer, (b) SU8-polydimethylsiloxane (PDMS)<sup>3</sup> casting and (c) PDMS-NOA63 casting. The idea behind it was to take advantage of the high resist thickness of up to  $75 \mu\text{m}$  and of the photolithographic structuring of SU8. SU8 process, for high aspect ratio and vertical sidewalls, established in our cleanroom by Miessner et al. [7]. An intermediate

\* Corresponding author.

E-mail address: [u.staufer@tudelft.nl](mailto:u.staufer@tudelft.nl) (U. Staufer).

<sup>1</sup> Norland, NOA63.

<sup>2</sup> Microchem, SU8 2025.

<sup>3</sup> Dow Corning, Sylgard 184 PDMS.

81 casting step in PDMS was necessary, to avoid bonding between SU8  
 82 and NOA63. The microfluidic system was completed by capping the  
 83 NOA63 trenches with a microscope glass-slide. This glass-slide allowed  
 84 an observation of the movement of fluorescently labeled  
 85 microspheres within the eo pump. In a purely NOA63 microfluidic  
 86 system, this would have been impossible since NOA63 exhibits high  
 87 fluorescent auto-emission at the wavelength of fluorescein [4,5]. To  
 88 facilitate the fluidic and electrical connections, Cord End terminals  
 89 were glued to the fluidic connections of the NOA63 cast.

90 The Ag/AgCl electrodes were, afterwards, electrolessly deposited  
 91 and structured into the closed capillaries of the microfluidic  
 92 system. According to Polk et al. [8], one of the major challenges  
 93 when integrating Ag/AgCl electrodes into microfluidic systems is  
 94 their poor stability due to dissolution of an only a few nanometer  
 95 thick AgCl layer. Additionally during eo pump actuation, the Ag/  
 96 AgCl electrode was continuously further transformed from Ag into  
 97 AgCl and vice versa. Hence, for a stable electrode and a long actuation  
 98 time, thick Ag/AgCl electrodes were required. In order to fabricate  
 99 them inside the NOA63/glass capillaries, an Ag deposition and a  
 100 subsequent transformation into AgCl, both using electroless  
 101 solutions, were chosen. To sufficiently increase the electrode thick-  
 102 ness, the electrodes were fabricated in a flow configuration [9], in-  
 103 stead of previously reported multiple depositions [6]. This had the  
 104 additional advantage that the concentration of the electroless solu-  
 105 tion could be kept constant throughout the capillary, as long as the  
 106 supply of reactants exceeded its loss due to the deposition reaction.

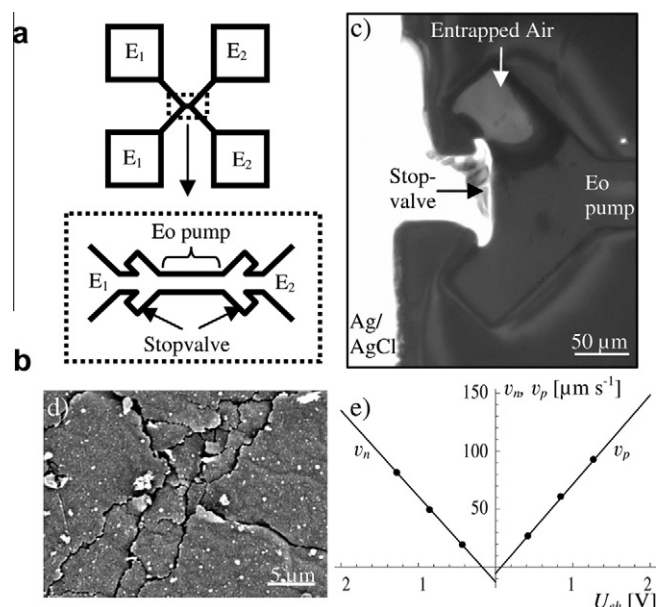
107 The Ag electrodes were fabricated from a Tollen's solution, simi-  
 108 lar to the one previously described [6]. The solution consisted of  
 109  $0.1 \text{ mol l}^{-1}$  silver nitrate,  $1 \text{ mol l}^{-1}$  ammonium hydroxide,  
 110  $0.1 \text{ mol l}^{-1}$  glucose and  $0.55 \text{ mol l}^{-1}$  sodium hydroxide. In contrast  
 111 to our previous report, neither sodium citrate was used, since the  
 112 reaction speed was decreased by setting the reaction temperature  
 113 to about  $20^\circ\text{C}$ , nor a silanization was required, since at these cross-  
 114 sections the adhesion of Ag to the surface was sufficient to create a  
 115 stable electrode. For the flow deposition, the solution was freshly  
 116 prepared and stored in a reservoir at  $3^\circ\text{C}$  to suppress the reaction.  
 117 From there, the solution was pumped within about 15 s through  
 118 silicone tubing to the chip. Each electrode was fabricated separa-  
 119 tely, hence the solution enters the microfluidic system through  
 120 one fluidic connection and exits through the corresponding second  
 121 microfluidic connection. The temperature and, hence, the deposi-  
 122 tion rate was expected to be constant throughout the chip, since  
 123 the solution was flushed comparatively fast through the chip with-  
 124 in 1 s. Microfluidic stopplaves were used at the entrance of the eo  
 125 pump for structuring the Ag electrodes, see Fig. 1b. The valves pre-  
 126 vented the filling of the eo pump with electroless solution. The  
 127 deposition was stopped by flushing with deionized water. More  
 128 details on the functionality and the design of the microfluidic stop-  
 129 plaves are given in Ref. [10].

130 Finally, the Ag electrodes were partially transformed into AgCl  
 131 by pumping a  $0.3 \text{ mmol l}^{-1}$  sodium hypochloride solution through  
 132 the capillary for 15 s. The reaction was again stopped by flushing  
 133 with deionized water. This transformation process was based on  
 134 the oxidation of the Ag layer by the hypochloride and an immedi-  
 135 ate precipitation of AgCl due to the presence of  $\text{Cl}^-$  ions.

### 136 3. Results and discussion

#### 137 3.1. Fabrication

138 Both casts, the PDMS master and the NOA63 trench, were demolded  
 139 by gently pulling off the structured SU8 layer or the PDMS  
 140 master, respectively. In both cases the master remained unaffected  
 141 and could be reused several times. A summary of the measured



142 Fig. 1. (a) Layout of the fluidic system with an embedded eo pump. (b) Detail of (a)  
 143 showing the eo pump and the electrodes ( $E_1$  &  $E_2$ ). The electrodes were structured  
 144 by microfluidic stopvalves. (c) Optical microscope image of a successful Ag  
 145 electrode deposition & structuring with a microfluidic stopvalve. During the  
 146 subsequent filling with water an airbubble was entrapped in a pocket of the  
 147 stopvalve. (d) Scanning electron image of a crack formation during the electroless  
 148 transformation from Ag into AgCl. (e) Average velocity  $v_m$  of the microspheres as a  
 149 function of the electrohydrodynamic voltage  $U_{ch}$  drop over the eo pump.

142 NOA63 cast dimensions were: (a) an electrode capillary: length  
 143 from microfluidic connection to eo pump 3.5 mm, cross-section  
 144  $395 \mu\text{m} \times 65 \mu\text{m}$  and (b) an eo pump: length  $l_p = 600 \mu\text{m}$ , cross-  
 145 section  $w_p = 65 \mu\text{m} \times h_p = 55 \mu\text{m}$ .

146 From optical observations, it was concluded, that the Ag layer  
 147 homogeneously deposited inside the capillary, except at the contact  
 148 points to the Cord End terminals. The measured conductance  
 149 between the Cord End terminals was 0.25 s. At the contact points  
 150 to the Cord End terminals, the reaction was decreased and the  
 151 gap between the contact and the electrode closed only slowly dur-  
 152 ing the deposition. This locally slower growth was explained by the  
 153 high sensitivity of the Ag deposition on contamination. The thinner  
 154 contact reduced the overall conductance as measured between the  
 155 two Cord Ends. This made an estimation of the Ag layer thickness  
 156 not very reliable. A successful Ag electrode deposition and struc-  
 157 turing can be seen in Fig. 1c. The Ag layer can be seen as the highly  
 158 reflective and bright surface on the left side of the optical micro-  
 159 scope image.

160 The transformation of the Ag into the AgCl electrode was chal-  
 161 lenging since the electrode tended to delaminate or crack, as e.g.  
 162 shown in Fig. 1d. The growth of AgCl resulted in compressive stress  
 163 in the electrode due to the lower molar density of AgCl  
 164 ( $38 \text{ mmol cm}^{-3}$ ) than Ag ( $97 \text{ mmol cm}^{-3}$ ) based on values taken  
 165 from Atkins et al. [11], General Chemistry, and Cain et al. [12].  
 166 In the progress of many deposition and AgCl transformation exper-  
 167 iments, it turned out that a mechanically stable Ag/AgCl electrode  
 168 could be fabricated by limiting the transformation to 20% of the  
 169 initial Ag layer thickness.

170 The experiments performed with the electrode lasted in the  
 171 range of 5 min at currents of  $1 \mu\text{A}$ . During this time no significant  
 172 electrode deterioration was observed. However, applying an exces-  
 173 sive voltage of 10 V and above caused the dissolution of white  
 174 flakes, probably patches of AgCl, and the onset of undesired  
 175 hydrolysis.

### 3.2. Flow measurement

The eo flow was determined by measuring the velocity of fluorescently labeled monodisperse carboxylated microspheres<sup>4</sup> of radius 0.7  $\mu\text{m}$  dispersed in a test-solution of 10  $\text{mmol l}^{-1}$  potassium chloride (KCl) and 2  $\text{mmol l}^{-1}$  tris(hydroxymethyl)aminomethane, at a pH of 10 adjusted with NaOH. The solution was freshly prepared before each experiment and its specific conductivity was measured to be  $\sigma_s = 0.197 \text{ Sm}^{-1}$ . For the electrokinetic flow measurements, the chip with the eo pump was mounted with the glass-slide towards an inverted fluorescent microscope<sup>5</sup> and voltages in the range up to 5 V were applied at the Cord End terminals.

The average velocity  $v$  of the microspheres was measured as a function of the voltage drop over the eo pump  $U_{eh}$ , shown in Fig. 1e. The average velocity of six microspheres was taken, at different positions within the capillary cross-section. The microsphere's velocity  $v$  was split into two parts for better illustration,  $v_n$  and  $v_p$  for negative and positive applied voltage  $U_{eh}$  drops over the eo pump, respectively. The linear fit of the microsphere velocity was determined to be  $v_n = 74 \mu\text{m s}^{-1} \text{V}^{-1} |U_{eh}| - 12.8 \mu\text{m s}^{-1}$  and  $v_p = 77 \mu\text{m s}^{-1} \text{V}^{-1} U_{eh} - 5.4 \mu\text{m s}^{-1}$ . From this result, it was speculated that the difference in the offset of the velocities  $v_{hy,p} = -7.4 \mu\text{m s}^{-1}$  at  $U_{eh} = 0 \text{ V}$  was caused by a remaining hydrostatic pressure difference. The hydrostatic pressure induced flow was calculated to be  $Q_{hy} = 26 \text{ pl s}^{-1}$ , which equaled an average height difference of the solution level in the two electrode reservoirs of 6.1  $\mu\text{m}$ . The slope of the microsphere velocities  $v_n$  and  $v_p$  was not significantly different, which was a good indicator of a similar transformation into AgCl for both electrodes. Using the average offset at  $U_{eh} = 0 \text{ V}$  and the average microsphere velocity  $v_m$ , lead to an offset in the voltage drop over the eo pump  $U_{eh}$  of 0.12 V. This slight offset was expected to be caused by the electrochemical reaction at the electrode.

The average electrokinetic contribution of the microsphere's velocity  $v_m$  was calculated to be  $v_m = 75 \mu\text{m s}^{-1} \text{V}^{-1} U_{eh}$ . The velocity  $v_m$  of the carboxylated microspheres was the result of two electrohydrodynamic effects: the voltage drop  $U_{eh}$  over the eo pump induced an eo flow of the test solution in the capillary and an electrophoretic (ep) movement of the microspheres itself. In order to extract and estimate the contribution of the eo flow, the eo mobility  $\mu_{eo}$  needed to be determined, the latter correlates to the zeta-potential  $\zeta$  of the charged capillary surface. In the presented case, the capillary consisted of a glass capped NOA63 trench. The zeta-potential  $\zeta_{gl}$  of the glass-slide was expected to be in the same range, as reported by Scales et al. [13], for a 10  $\text{mmol KCl}$  solution on a fused silica glass capillary, at pH 10,  $\zeta_{gl} = -74 \text{ mV}$ . However, the usage of NOA63 for microfluidic devices is a recent development and not many experimental results on the eo mobility  $\mu_{eo}$  are available in literature. It is known that NOA63 is based on polyurethane [14]. We approximate, therefore, the zeta-potential  $\zeta_{NOA63}$  for the NOA63 surface with that of a polyurethane surface. This represents only a rough estimate, since the NOA63 surface charge  $\sigma_{ch}$  might be strongly influenced by any eventual functional sidegroups as well as by the degree of polymerization. Voigt et al. [15], investigated the zeta-potential  $\zeta$  of a polyurethane surface<sup>6</sup> for pH values up to 9 at a NaCl concentration of 1  $\text{mmol l}^{-1}$ . In their experiments, it can be seen that the zeta-potential  $\zeta$  remained relatively constant, around  $-50 \text{ mV}$  from pH 6 to  $-55 \text{ mV}$  at pH 9. Hence, we assumed that the zeta-potential  $\zeta_{NOA63}$  at pH 10 could be approximated by a value of  $-55 \text{ mV}$ . For a low concentration  $c$  of counter ions, the zeta-potential  $\zeta$ , depending on this concentration

$c$ , can be approximated by  $\zeta \sim -\log c$  [16]. This resulted in an estimated zeta-potential of the NOA63 surface exposed to the test solution of  $\zeta_{NOA63} = -36 \text{ mV}$ . The average zeta-potential  $\zeta_{cs}$  for the capillary surface was determined by the weighted fraction of the cross-sectional perimeter to  $\zeta_{cs} = [\zeta_{gl}W + \zeta_{NOA63}(2d + w)]/(2d + 2w) = -48 \text{ mV}$ . The eo mobility  $\mu_{eo}$  was determined to:

$$\mu_{eo} = \frac{\epsilon\epsilon_0\zeta_{cs}}{\eta} = -3.3 \times 10^{-8} \text{ m}^2 \text{ V}^{-1} \text{ s}^{-1}, \quad (1)$$

where  $\epsilon\epsilon_0$  and  $\eta$  denote the dielectric constant of water ( $\epsilon = 78$ ) and the viscosity of water ( $\eta = 1 \text{ mPa s}$ ), respectively. According to Morf et al. [17], the eo induced flow in the microfluidic system can be described by:

$$Q_{eo} = U_{eh}\mu_{eo} \frac{R_{hy,p}}{R_{hy,e} + R_{hy,p}} \frac{wh}{l}, \quad (2)$$

where  $R_{hy,e}$  and  $R_{hy,p}$  denote the hydraulic resistance of the electrode and of the eo pump, respectively. With the eo mobility  $\mu_{eo}$  and the capillary's hydraulic resistances, the average eo velocity contribution to the microsphere velocity  $v_{eo}$  can be calculated. The average eo velocity  $v_{eo}$  contribution was calculated with Eq. (2), to:

$$|v_{eo}| = \frac{|Q_{eo}|}{wh} = 39 \mu\text{m s}^{-1} \text{V}^{-1} |U_{eh}|. \quad (3)$$

Behrens et al. [18], measured the ep mobility  $\mu_{ep}$  of carboxylated latex microspheres<sup>7</sup> to be  $\mu_{ep} = 6.5 \times 10^{-8} \text{ m}^2 \text{ V}^{-1} \text{ s}^{-1}$  for a solution of 10  $\text{mmol l KCl}$  at pH 1. An ep experiment for a rough estimation, performed with the microspheres used in this research, indicated a similar ep mobility  $\mu_{ep}$ . Hence, the ep velocity  $v_{ep}$  contribution to the microsphere velocity was calculated to be:

$$|v_{ep}| = \frac{|\mu_{ep}U_{eh}|}{l} = 108 \mu\text{m s}^{-1} \text{V}^{-1} |U_{eh}| \quad (4)$$

The contribution of the eo velocity and ep velocity need to be combined to obtain the actual velocity of the microspheres, with respect to a stationary capillary. Both surfaces, the surface of the chip and the surface of the microspheres, were negatively charged. This resulted in an opposing effect of electroosmosis and electrophoresis. The resulting velocity  $v_{mm}$  of the microspheres was calculated to:

$$v_{mm} = (v_{ep} - v_{eo})U_{eh} = 69 \mu\text{m s}^{-1} \text{V}^{-1} U_{eh}.$$

The direction of the velocity  $v_{mm}$  was defined in the same direction as the voltage drop over the eo pump  $U_{eh}$ . This estimated microsphere velocity was in good agreement with the measured average microsphere velocity of  $v_m = 75 \mu\text{m s}^{-1} \text{V}^{-1} U_{eh}$ . From that, the eo pump rate  $Q_{eo}$  was calculated from the measured average slope of the microsphere velocity  $v_m$ , as shown in Fig. 1e and corrected for an estimated ep velocity  $v_{ep}$  of  $108 \mu\text{m s}^{-1} \text{V}^{-1}$ . The eo pump rate  $Q_{eo}$  as a function of the voltage drop over the eo pump  $U_{eh}$  was calculated to be  $Q_{eo} = 0.12 \text{ nl s}^{-1} \text{V}^{-1} U_{eh}$ .

## 4. Summary and conclusions

A quick, easy and cheap fabrication of an eo pump with integrated Ag/AgCl electrodes was shown based on casting the hydrophilic polymer NOA63 and capping the trenches (hydraulic dimension in the range of 55  $\mu\text{m}$ ) with a glass-slide and a subsequent Ag/AgCl electrode deposition by flow of electroless solution and microfluidic structuring by stopvalves. The final eo pump was modeled and characterized by measuring the velocity of fluores-

<sup>4</sup> Polyscience, Flouresbrite YG Carboxylated Microspheres, diameter 1.5  $\mu\text{m}$ .

<sup>5</sup> Zeiss, Axiovert S40 with a mounted camera AxioCam Mrm and a metal halide lamp HXP 120.

<sup>6</sup> VEB, SYSpur.

<sup>7</sup> Interfacial Dynamics Cooperation, radius of 155 nm

cent carboxylated microspheres inside the eo pump. From that, the eo flow rate of the low voltage pump was determined to be  $Q_{eo} = 0.12 \text{ nl s}^{-1} \text{ V}^{-1} U_{eh}$ .

The integration of Ag/AgCl electrodes into the microfluidic system reduced the footprint of the eo pump, since hydrolysis is suppressed at this specific kind of electrodes and elements for liquid gas separation were not required. Furthermore, the integration reduced the length of the eo pump, hence, commonly applied voltages in the range of kV were reduced down to a few Volts. The presented eo pump design, fabrication and analysis represents a promising strategy towards a high density integration of micro-pumps into a microfluidic system.

## References

- [1] S. Ghosa, *Electrophoresis* 25 (2004) 214–228.
- [2] Heuck et al., "Low voltage electroosmotic pump for high density integration into microfabricated fluidic systems", *Microfluidic and Nanofluidics*, in press.
- [3] Brask et al., *Lab on Chip* 5 (2005) 730–738.
- [4] Janz et al., *Annals of the New York Academy of Science* 148 (1968) 210–221.
- [5] Dupont et al., *Microelectronic Engineering* 87 (2010) 1253–1255.
- [6] Heuck et al., *Microelectronic Engineering* 87 (2010) 1383–1385.
- [7] Miessner et al., *Proceedings 14th Symposium of Laser Techniques to Fluid Mechanics*, 2008.
- [8] Polk et al., *Sensors and Actuators B* 114 (2006) 239–247.
- [9] Kenis et al., *Accounts of Chemical Research* 33 (2000) 841–847.
- [10] Heuck et al., "Electroless Deposition and Structuring of Silver Electrodes in Closed Microfluidic Capillaries", *Journal of Microelectromechanical Systems*, in press.
- [11] Atkins et al., *General Chemistry*, Freeman and Company press, 1992.
- [12] Cain et al., *Journal of Physics and Chemistry of Solids* (1980) 173–178.
- [13] Scales et al., *Langmuir* 8 (1992) 965–974.
- [14] Kim et al., *Advanced Functional Materials* 17 (2007) 3493–3498.
- [15] Voigt et al., *Biomaterials* 4 (1983) 299–304.
- [16] Kirby et al., *Electrophoresis* 25 (2004) 203–213.
- [17] Morf et al., *Sensors and Actuators B* 72 (2001) 266–272.
- [18] Behrens et al., *Langmuir* 16 (2000) 2566–2575.

Q2 312  
313  
314  
315  
316  
317  
318  
319  
320  
321  
322  
323  
324  
325  
326  
327  
328  
329  
330  
331  
332  
333